

Relaxation Kinetics of an L_3 (Sponge) Phase

T. D. Le,^{*,†,‡} U. Olsson,[‡] H. Wennerström,[‡] P. Uhrmeister,[§] B. Rathke,[§] and R. Strey[§]

Center for Chemistry and Chemical Engineering, Physical Chemistry 1, Lund University, P.O. Box 124, SE-221 00 Lund, Sweden, and Institut für Physikalische Chemie, Universität zu Köln, Luxemburger Strasse 116, D-50939 Köln, Germany

Received: January 18, 2002; In Final Form: June 14, 2002

The kinetic response of an L_3 (sponge) phase formed in the $C_{12}E_5$ – n -decane–brine system is studied using the Joule-heating temperature jump (JHTJ) technique. The equilibrium state of the spongelike membrane is instantaneously perturbed, and the kinetic response is monitored using a multi-angle light scattering setup. These measurements yield a time-dependent scattering intensity as a function of temperature, scattering vector q , and concentration. We observed a single-exponential relaxation characteristic time, τ_m . The q dependence of the scattering amplitude shows an Ornstein–Zernike behavior, but we can identify two concentration regimes with respect to the relaxation behavior. For volume fractions $\Phi_m = 0.20$, there is no detectable q dependence of the relaxation times, while for samples with $\Phi_m > 0.30$, the relaxation times display the q^{-2} dependence typical of a diffusive process and with relaxation times consistent with those found in dynamic light scattering. At the intermediate concentrations, there is a transition from the q -independent to the q^{-2} dependence behavior. Analysis from each concentration regime reveals distinct differences in the dependence of τ_m on temperature and concentration, with an extraordinarily strong concentration dependence of τ_m ($\tau_m \approx \Phi^{-9}$) in the low concentration regime and a temperature dependence corresponding to a formal Arrhenius activation energy of 720 kJ/mol or 275 kT.

1. Introduction

The sponge or L_3 phase consists of a surfactant or surfactant–solute bilayer extending in a three-dimensional, multiply connected network.^{1–3} The phase is isotropic and has a characteristic stability range appearing as a narrow band in a phase diagram. This phase can appear over a large concentration range provided that one adjusts some intensive variable, such as temperature. Figure 1 shows a partial phase diagram of the system $C_{12}E_5$ –decane–water with the surfactant-to-oil ratio used in the present study. For this system, the temperature dependence of the phase equilibria is due to the temperature sensitivity of the spontaneous curvature.⁴

The basic driving force for the formation of the complex bilayer topology of the sponge phase is to obtain a match between the spontaneous and the mean monolayer curvature.^{5,6} This imposes an extra constraint on the system, and such a match can optimally be obtained only in a narrow concentration range.

It is now well-established that the basic structure of the sponge phase consists of a multiply connected bilayer. Less, however, is known about the kinetic properties of the bilayer membrane. Sponge phases show in general a low zero-shear viscosity.⁷ A Newtonian behavior is often observed, although a structural transformation to a planar lamellar structure can be induced at higher strain rates.⁸ Waton and Porte⁹ reported on a temperature jump study of a sponge phase made up of ionic surfactant, cosurfactant, and brine. A somewhat complex response was observed with different relaxation processes. More recently,

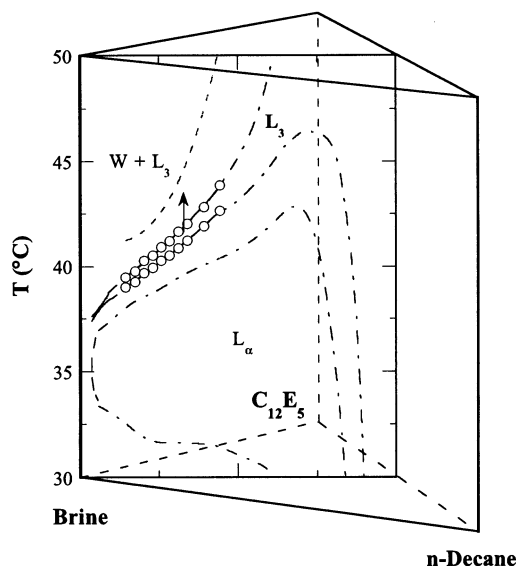


Figure 1. Phase diagram of an L_3 phase formed in the $C_{12}E_5$ – n -decane–brine system. The T – Φ plane shown is at fixed surfactant-to-oil ratio ($\Phi_s/\Phi_o = 0.815$). The L_3 phase coexists with a lamellar, L_a , phase at lower temperatures and a dilute solution, W , phase at higher temperatures. Temperature jumps were made in successive ΔT steps from an equilibrium L_3 phase marked by the symbol (O).

Schwarz and co-workers¹⁰ investigated a nonionic system using several relaxation techniques. In particular, they found consistency between temperature and pressure jump data and a much simpler relaxation behavior than that in the study of Waton and Porte. The relaxation could in this case be described by a single relaxation time, but showed a very strong dependence on both the concentration and temperature. The relaxation time decreased

* To whom correspondence should be addressed. E-mail: Thao.Le@GensiaSicor.com.

[‡] Lund University.

[†] Present address: Gensia Sicor Pharmaceuticals, 19 Hughes, Irvine, CA 92618.

[§] Universität zu Köln.

with increasing concentration approximately as Φ^{-9} , where Φ is the bilayer volume fraction.

In this paper, we report on the kinetics of the system C₁₂E₅–*n*-decane–brine using the Joule-heating temperature jump (JHTJ) technique whereby the kinetic response is monitored via the light-scattering properties. The system is similar to that investigated by Schwarz et al., but here the surfactant bilayer is swollen by the decane. An important reason for choosing this system is that its equilibrium thermodynamic and bilayer elastic properties have been determined previously. Although the stability range of the sponge phase for this system is narrow for a fixed concentration, between 0.5 and 1.2 °C,¹¹ we have found in the same system using static light scattering that there are substantial variations (up to 50%) of the osmotic compressibility across this narrow range.¹² The correspondingly strong temperature dependence of the scattered light intensity ensures a detectable response to a temperature jump perturbation.

2. Experimental Section

Materials and Preparation Procedures. Pentaethylene glycol dodecyl ether, C₁₂E₅ (Nikkol Ltd.), *n*-decane (Sigma-Aldrich Chemie GmbH), and NaCl–“Titrisol” (Merck) have purity better than 99% and were used without further purification. The samples were prepared by diluting a stock mixture of C₁₂E₅/*n*-decane (51.9/48.1 wt %) with a stock mixture of 0.1 M NaCl solution. Conversion from weight to volume fraction was done using the following densities: 0.967 g/cm³ (C₁₂E₅), 0.730 g/cm³ (*n*-decane), 2.165 g/cm³ (NaCl), and 0.997 g/cm³ (Millipore filtered water). The membrane (bilayer) volume fraction of the present system is defined as $\Phi_m = (0.5\Phi_s + \Phi_o)$, and the bilayer half-thickness is defined as $l = l_s(\Phi_m/\Phi_s)$, where l_s (14.5 Å) is the surfactant length¹³ and Φ_s and Φ_o are the surfactant and oil volume fractions, respectively.

The samples were thoroughly mixed in the L₁ (microemulsion) phase, a transparent solution near room temperature. The sample tubes were then placed in a thermostatic water bath and allowed to equilibrate at an L₃ phase temperature. The L₃ phase coexists with a lamellar phase, L_α, at lower temperatures and a dilute solution (essentially pure water) phase, W, at higher temperatures. These coexistence boundaries were determined with an accuracy of ±0.05 °C by visual examination between crossed polarizers in a water bath.

A thermostated syringe was used to transfer the sample into the scattering cell of the *T*-jump apparatus.^{14,15} During the transfer, an attenuated light source was used to ensure that the sample remained homogeneous; the temperature of the scattering cell was kept constant to within ±0.02 °C. Further details of the *T*-jump setup and calibration can be found in ref 11.

Joule-Heating Temperature Jump (JHTJ). The temperature (*T*) jump technique used in this study is of the type Joule pulse heating (JHTJ). The *T*-jump setup consists of a high-voltage capacitor (DIA-RHD from Dialog), a laser source with a wavelength $\lambda_o = 532$ nm and variable power settings (Millenia II from Spectra-Physics), here fixed at 0.2 W, five photomultipliers (two DIA-PMF from Dialog and three H5784-01 from Hamamatsu) placed at five different angles (40°, 60°, 90°, 120°, and 140°) with respect to the incident laser, and two photodiodes (OSI 5K from Laser Components) for monitoring the turbidity of the sample. The measurements yield the time-dependent scattering intensity at five scattering vectors, $q = 4\pi n/\lambda_o \sin(\theta/2)$, where λ_o is the wavelength of the laser, θ is the scattering angle, and n is the refractive index of the sample.

The principle behind this setup is to instantaneously perturb the equilibrium state of a sample, located between Pt plates, by

means of discharging a high-voltage capacitor. The temperature jump, ΔT , generated by the pulse can be calculated using the relation¹⁶ $\Delta T = CU^2/(2Q)$, where C is the capacitance (10 nF), U is the charging voltage of the capacitor, and Q is the total heat capacity of the sample. The parameter Q contains the effective cell volume (V_{eff}), specific heat (c_p), and density (ρ) of the sample. The latter two variables are expected to change with the composition of the sample; that is, with increasing concentration of surfactant and oil, Φ_{s+o} , c_p will increase while ρ will decrease. To calibrate the instrument we used the microemulsion phase, L₁, of the same system, with the same Φ_{s+o} ratio, and measured the jump temperature, ΔT , as a function of the voltage used to charge the capacitor, U_{cap} , at various Φ_{s+o} . For a range of concentrations, we find that ΔT varies linearly with Φ_{s+o} and used the empirical relationship, $C/(2Q) = (4.0 + 15.4\Phi_{s+o})10^{-9}$ °C V⁻², to determine the concentration dependence of the jump temperature in the L₃ phase.

The rapid (exponential) heating time was calculated using $\tau_h = RC/2$, where R is the resistance of the sample. The resistance was measured with a precision component analyzer (model 6425 from Wayne Kerr) for each sample. The experimental conditions (e.g., 0.1 M NaCl, sample system, cell geometry) resulted in a characteristic heating time of $\tau_h = 2.7 \pm 1$ μs. This heating time is several orders of magnitude faster than the cooling time of the cell ($\tau_c = 18$ s, see below) and also faster than the relaxation of the system being investigated.¹¹

The temperature after a jump, T_j , is the sum of the initial temperature and the jump step, $T_i + \Delta T$. A range of ΔT between 0.08 ± 0.01 and 1.47 ± 0.12 °C can be accessed for the present system, in which reasonable signal-to-noise ratio was achieved. Details of the setup and data treatment are provided in ref 11.

Dynamic Light Scattering (DLS). Dynamic light scattering (DLS) measurements were performed on a commercial ALV goniometer setup (Lange) equipped with an ALV-5000 multiple digital correlator and a 50 mW He/Ne laser ($\lambda_o = 632.8$ nm). This setup can access a range of angles between 30° and 150°, and the temperature stability is within ±0.02 °C. The commercial software CONTIN was used to analyze the data. Details of the setup are provided in ref 17.

3. Results

Sponge Phase. Figure 1 shows a phase diagram displaying the narrow sponge (L₃) phase of the C₁₂E₅–*n*-decane–brine system at the fixed surfactant/oil ratio, $\Phi_s/\Phi_o = 0.815$. For a given concentration, the L₃ phase coexists with a lamellar (L_α) phase at lower temperatures and a dilute solution (W) phase at higher temperatures. As noted in the Experimental Section, 0.1 M NaCl solution was used to increase the conductance in the continuous (aqueous) medium. The presence of the salt was observed to consistently lower the phase boundaries by 0.9 °C.¹¹ We have studied the relaxation behavior at 10 concentrations in the interval $0.11 \leq \Phi_m \leq 0.39$. Although the sponge phase is stable over a larger concentration interval, measurements at concentrations lower than $\Phi_m = 0.11$ were uninformative because the sample relaxation time was longer than the thermal cooling time. Conversely, for $\Phi_m > 0.34$, the relaxation time τ_m becomes shorter than the lower time resolution limit, $\sim 10^{-4}$ s, of the instrument. This limit is determined by the A/D converters using a minimum of 20 ms to scan 1024 data points from the photodiodes.

The initial temperatures, T_i , were inside the equilibrium one-phase region, and the size of the *T* jump was varied such that the final temperature, $T_j = T_i + \Delta T$, is either within the one-

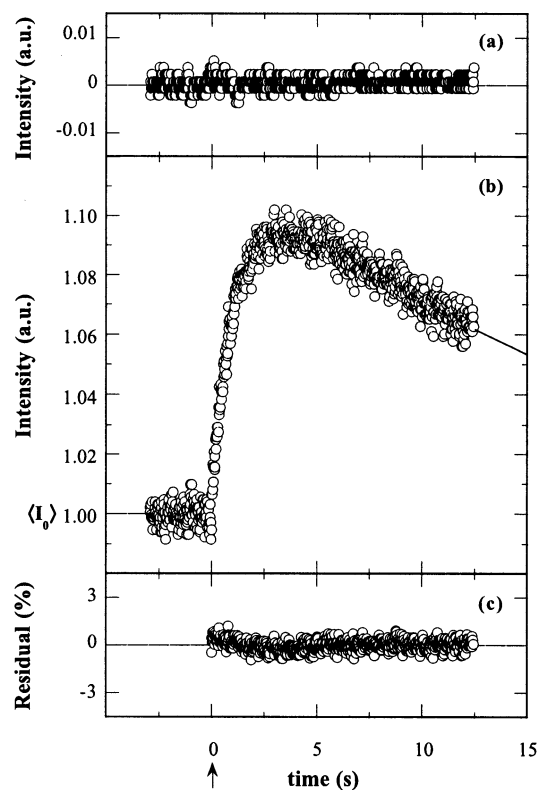


Figure 2. Sample data treatment. The example shown is for a $\Phi_m = 0.11$ sample measured at 140° angle: (a) laser; (b) T jump from 39.16 to 39.42 $^\circ\text{C}$; (c) residual from fit.

phase area or slightly outside. We observe qualitatively the same relaxation behavior independent of the jump size as long as there is no nucleation of water droplets during the transient. This phase separation process puts an upper temperature limit on the size of the temperature jump. The dashed line shown in Figure 1 marks the observed upper limit of the experiments, which is never more than 1.5 $^\circ\text{C}$ outside the one-phase area.

Light-Scattering Response in the JHTJ Experiments. The photomultipliers (PM) and photodiodes (PD) in this setup allowed for simultaneous monitoring of the intensity change at different angles during the T jump. The intensity change as a function of time, shown in Figure 2, is characterized as¹¹

$$I(t) = I(T_i) + \frac{I(T_j) - I(T_i)}{1 - \tau_m/\tau_c} [\exp(-t/\tau_c) - \exp(-t/\tau_m)] \quad (1)$$

where $I(T_i)$ and $I(T_j)$ are the intensities at T_i and at T_j , respectively, and τ_m and τ_c are the relaxation time of the membrane and cooling time of the instrument, respectively. Our experimental conditions yield a characteristic cooling time of the cell $\tau_c = 18$ s.¹¹ With the independently determined values of τ_c and $I(T_i)$ substituted into eq 1, there remain only two parameters, τ_m and $I(T_j)$, to be fitted. These parameters provide separate pieces of information on the sampling system and, thus, can be examined separately.

In this paper, we focus only on τ_m , the kinetics of membrane relaxation. The scattering intensity has been examined in detail in ref 11. Considering that for each starting temperature jumps were made between eight and 17 different final temperatures and that the light scattering intensity was monitored at five different angles, we have in all a collection of several hundred different sets of relaxation data. The majority of these showed the simple behavior as illustrated in Figure 2, which can be accurately fitted with a biexponential form. With the cooling

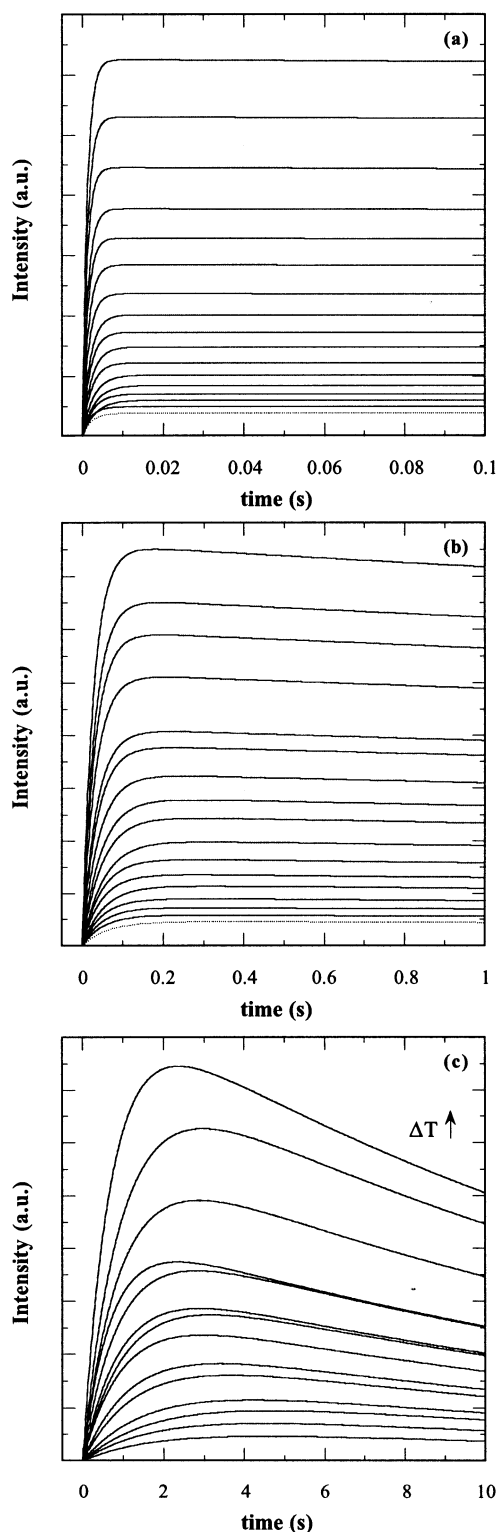


Figure 3. Fitted results from the samples with $\Phi_m =$ (a) 0.20, (b) 0.16, and (c) 0.11 measured at 90° angle jumping from initial temperatures 40.50, 39.79, and 39.16 $^\circ\text{C}$, respectively. Note the variation of the relaxation kinetics with concentration.

time τ_c constrained to be equal for the entire data set, we extract only a single system-dependent relaxation time, τ_m . Note that for the experiments reported here there are at least an order of magnitude difference between τ_c and τ_m ; thus, a slight variation in τ_c is expected to have an insignificant impact on τ_m . In Figure 3a–c, we show representative fitted relaxation behavior at three concentrations and each with 15 values of ΔT . Note the variation in the time scale of the relaxation process.

As mentioned above, the light-scattering response after a T jump follows the relation given by eq 1 for the majority of samples. The relaxation time τ_m decreases strongly with increasing concentration (see below), and for higher concentrations, the cooling time could be neglected in the time window of the experiment. The simple relation of eq 1 was, however, not found to hold in an intermediate concentration range (approximately $0.22 < \Phi_m < 0.30$). In this range, the light-scattering response is nonmonotonic with intensity overshoots and, in some instances, oscillations are also observed. Thus, we can divide the concentration range studied into three different intervals that from here on will be labeled as regions I, II, and III. In region I ($\Phi_m = 0.22$) and region II ($\Phi_m = 0.3$) the light scattering responses are monotonic and exponential, respectively. These regions are however separated by a crossover regime (region III) where a nonmonotonic response is observed. The situation is illustrated in Figure 4a–c, in which an example of the light scattering response from each of the three regions is compared. Relaxation times, τ_m , were only evaluated in regions I and II.

T Jump from Different Initial Temperatures. It is important to check to see whether the relaxation kinetics depend on the initial temperature of the jump, T_i . For five concentrations, we performed two to three series of measurements jumping from different initial temperatures but to the same final temperature. In all cases, we found that the relaxation time τ_m is the same irrespective of the starting temperature. An example of the data from a $\Phi_m = 0.11$ concentration is shown in Figure 5.

Angular Dependence. With measuring devices positioned around the sample, we could detect the scattering intensity at different angles corresponding to different scattering vectors, $q = 4\pi n \sin(\theta/2)/\lambda_o$, where $n = 1.33 + 0.11\Phi_{s+o}$ and $\lambda_o = 532$ nm. For each concentration, we have six independent measurements of τ_m at each T -jump step, ΔT . Five of these provide τ_m at five different scattering vectors, q , and the sixth is a turbidity measurement, which is an average value over the full q range. The q dependence is an important consideration because it may provide further insights into the dynamic process governing the relaxation.

In region I ($\Phi_m = 0.22$), we found τ_m to be independent of the scattering vector q . Figure 6 shows one such example in which τ_m measured at one q value and from the response of the transmitted light yield essentially the same results. In region II ($\Phi_m \geq 0.3$), on the other hand, a q^{-2} dependence of the relaxation time was detected. Figure 7 compares the q dependence in two T jumps from regions I and II, respectively. The q^{-2} dependence observed in region II is typical of a diffusive process, and the relaxation times were found to be equal, within experimental error, to those found in dynamic light-scattering (DLS) experiments, that is,

$$\tau_D(q) = \frac{1}{D_c q^2} \quad (2)$$

where D_c is the collective diffusion coefficient and τ_D is the relaxation time of the density fluctuations. Figure 8 shows an example of DLS from a $\Phi_m = 0.157$ sample at 39.85 °C.

Concentration Dependence. One way to compare the relaxation times from different experiments is to make a comparison at one q value and a common temperature. Measurements made by T jump and DLS were extrapolated to $q = 2.27 \times 10^{-3} \text{ \AA}^{-1}$ ($\theta = 90^\circ$) and extrapolated, when necessary, to 41 °C and are shown in Figure 9. Labeled in different symbols are the q -independent and q^{-2} -dependent

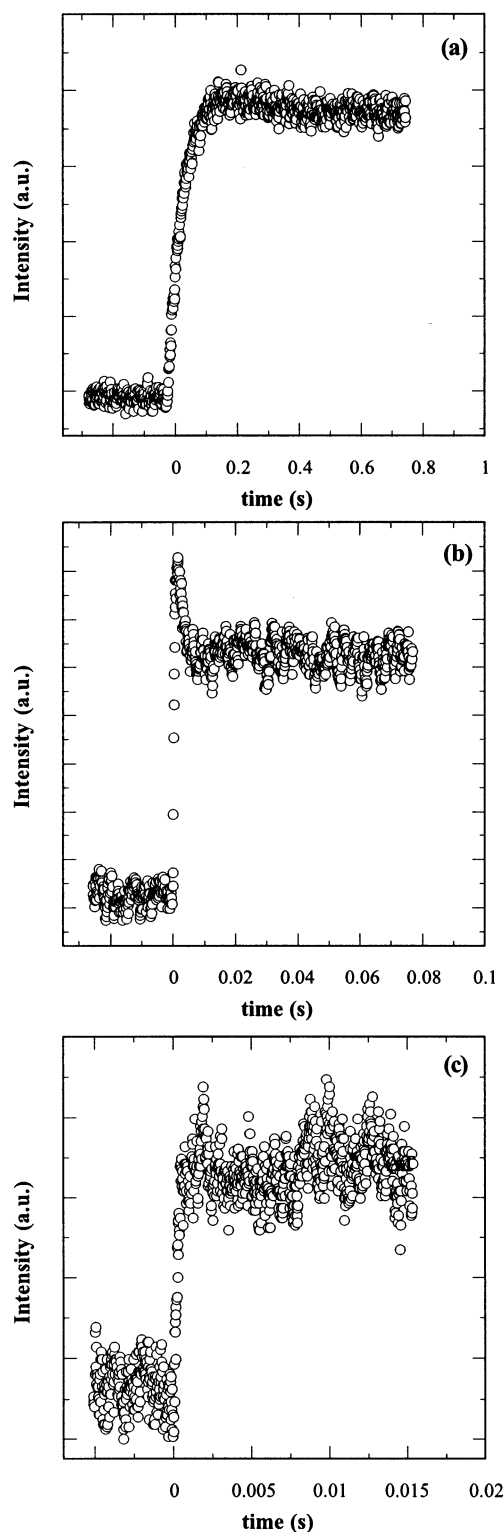


Figure 4. Intensity vs time curves measured at 40° angle in different concentration regimes: (a) region I, $\Phi_m = 0.16$, $\Delta T = 0.51$ °C; (b) region III, $\Phi_m = 0.26$, $\Delta T = 0.49$ °C; (c) region II, $\Phi_m = 0.34$, $\Delta T = 0.48$ °C.

relaxation times, in regions I and II, respectively. There is a spectacular concentration dependence of the relaxation times in region I, which vary by a factor of nearly 1000 for a 2-fold change in the concentration, but less dramatic concentration dependence at higher concentrations in region II. The different q dependencies and the different concentration dependencies of the relaxation times suggest that we observe different processes in the two regions. The data from T jump and DLS

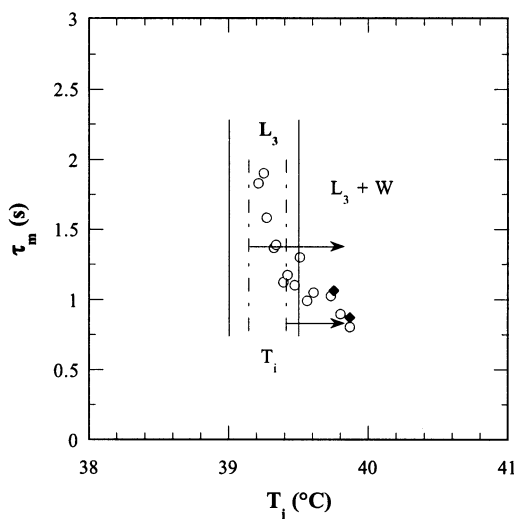


Figure 5. Relaxation time vs final temperature of a $\Phi_m = 0.11$ sample measured at two different initial temperatures: (○) $T_i = 39.16$; (●) $T_i = 39.41$ °C. The overlap of the data suggests that the relaxation time is independent of the initial temperature.

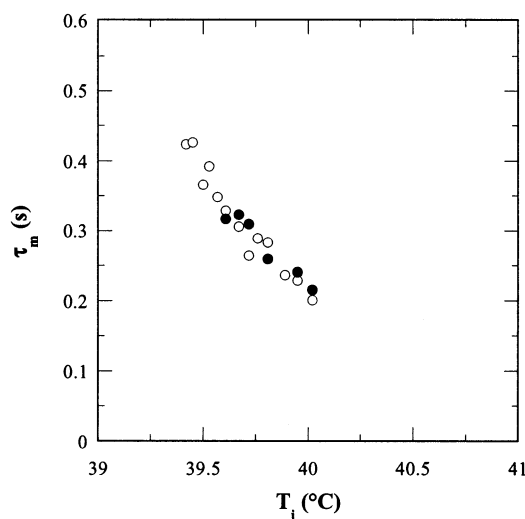


Figure 6. Relaxation kinetics of a $\Phi_m = 0.14$ sample jumping from a temperature of 39.33 °C: (○) 90° angle measurements; (●) turbidity measurements. The overlap of the data indicates that τ_m is independent of the scattering vector q .

closely matched one another in region II and can qualitatively be characterized as

$$\tau_m = \tau_D \propto \Phi_m^{-1} \quad (3)$$

If we continue the same line of thought and evaluate the Φ_m dependence of the relaxation time in region I in terms of a power law, this yields an extreme value for the exponent in the low-concentration range

$$\tau_m \propto \Phi_m^{-9} \quad (4)$$

Similar exponent has been found in a related system, $C_{10}E_4$ – n -decanol–water.¹⁰

From the combined findings of the q dependence and concentration dependence of τ_m , it is clear that diffusion is the rate-determining process, $\tau_m \propto q^{-2}$ and $\tau_m = \tau_D$, in region II. The behavior in region I is the most striking and will be discussed in more detail below.

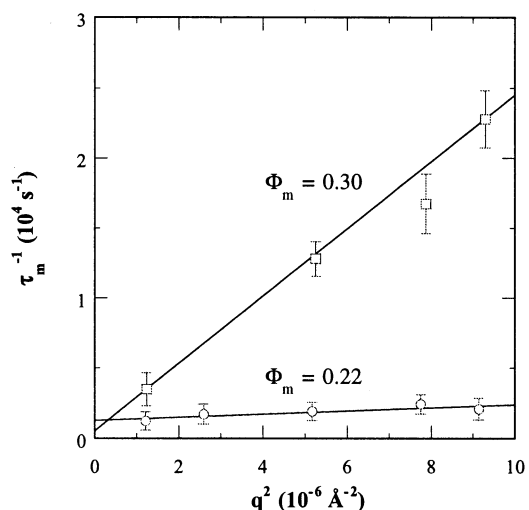


Figure 7. Plot of τ_m^{-1} vs q^2 . There is minor q dependence at $\Phi_m = 0.22$, which progressively increases with concentration. The examples shown are $\Phi_m = 0.22$ and 0.30 measured at 41.26 and 43.22 °C, respectively.

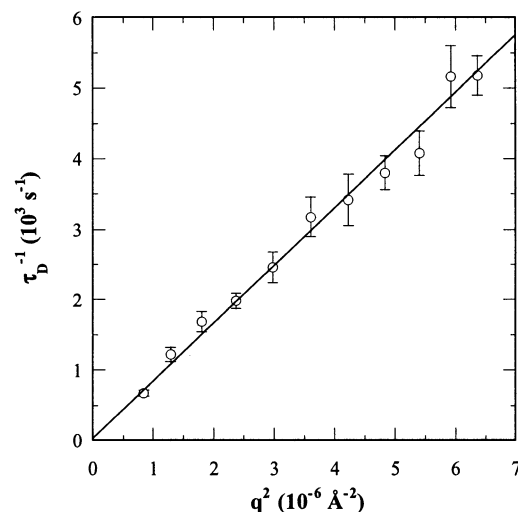


Figure 8. Dynamic light-scattering results from a $\Phi_m = 0.16$ sample measured at 39.85 °C.

Activation Energy in Region I. We have experimentally confirmed that τ_m depends only on the final temperature of the T jump, T_j . Over the narrow temperature range available, the data are consistent with an Arrhenius behavior,

$$\ln(\tau_m) = \ln(\tau_0) + \Delta E/(kT) \quad (5)$$

where τ_0 is the pre-exponential factor and ΔE is the activation energy. Shown in Figure 10 are best-fits of the data using eq 5, and within the experimental accuracy, we find that ΔE is independent of the concentration in region I and

$$\langle \Delta E \rangle = 1.2 \times 10^{-18} \text{ J} \quad (275 \text{ kT at } 314 \text{ K}) \quad (6)$$

4. Discussion

For the present $C_{12}E_5$ –decanol–water system, we observe in two concentration regimes a monotonic relaxation from the initial equilibrium state toward the scattering intensity of the final state, which coincides with the equilibrium scattering intensity for the cases in which the final temperature is within the one-phase area. Within experimental accuracy, the relaxation can be described by a single relaxation time. However, the two

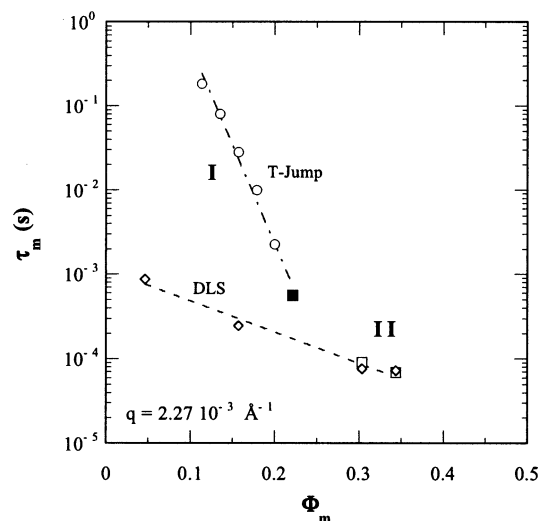


Figure 9. Dependence of τ_m on the concentration. Shown are the T -jump data (regime I, \circ , and regime II, \square) extrapolated to 41 °C, the averaged temperature of the L₃ phase in the concentration range investigated. Note that at $\Phi = 0.22$ (\blacksquare) the q dependence is minor, which progressively increases with concentration, cf Figure 7. The DLS data (\diamond) are at the equilibrium L₃ temperatures. As illustrated in Figure 1, the temperature range of the L₃ phase varies with concentration; hence, the minor temperature variation in the DLS measurements is reflected in the data at low concentration. An important observation here is the significant (orders of magnitude) variation with concentration.

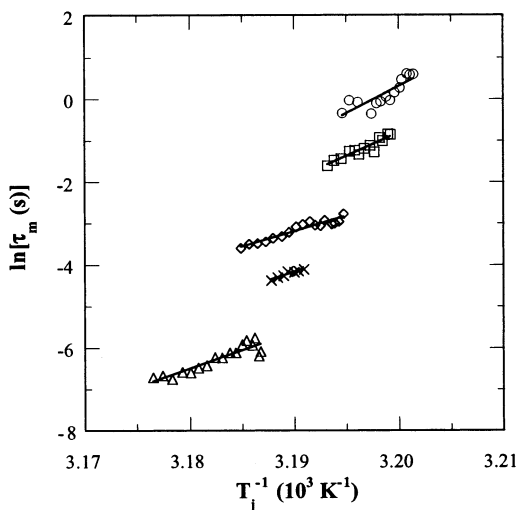


Figure 10. Arrhenius plot of the relaxation times. Shown are successive T jumps toward the L₃ + W domain for concentrations $\Phi = (\circ)$ 0.11, (\square) 0.14, (\diamond) 0.16, (\times) 0.18, and (\triangle) 0.20. Solid lines are best-fits using eq 5. A mean value of ΔE is found to be 275 kJ at $T = 314$ K.

separate concentration regimes show different kinetic behavior. This implies that two different relaxation processes are involved, one having the characteristics of a diffusion process. The regular behavior of the equilibrium properties suggests that the crossover is not due to some more fundamental change in the system. Rather, according to our present understanding of the sponge phase, the basic structure of the phase is concentration-independent apart from the fact that the structural length scale varies inversely proportionally to Φ_m .¹ This, together with the fact that the crossover appears to be continuous, suggests that both processes are operating in these two regimes, with the diffusional process as rate-determining at higher concentration while the other process is the rate-determining step at lower concentrations.

To identify the microscopic source of the second relaxation process, we make use of our understanding of the equilibrium properties of the system. The relaxation from the initial to the final state is monotonic, which is consistent with the minimal assumption that it reflects the relaxation of a microscopic/mesoscopic property from its initial equilibrium to the final (quasi)-equilibrium value. The temperature jump causes a jump in the spontaneous curvature, H_0 , and it is our understanding that H_0 is an important variable for determining the topology of the surfactant bilayer. The average Gaussian curvature, $\langle K_b \rangle$, of the bilayer midplane is related to the mean curvature of the surfactant monolayer, $\langle H \rangle$, evaluated at the polar–apolar interface, and for low values of the principal curvatures, we can write⁵

$$\langle K_b \rangle = \langle H \rangle / l \quad (7)$$

Here, l is the bilayer half-thickness, that is, the distance from the bilayer midplane to the polar–apolar interface, where we evaluate the curvature of the monolayer. The topology of a surface is often quantified in terms of the so-called Euler characteristic, χ_E , which according to the Gauss–Bonnet theorem¹⁸ is proportional to the integrated Gaussian curvature

$$\langle K_b \rangle A = 2\pi\chi_E \quad (8)$$

where A is the interfacial area.

For nonionic ethylene oxide-based surfactants, H_0 decreases with increasing temperature. This is the driving force for the lamellar-to-sponge transition with increasing temperature. If $\langle H \rangle$ in the L₃ phase continues to respond to changes in H_0 , we consequently expect that a temperature jump will induce a topology change. The temperature dependence of H_0 has been found to be linear over a large temperature interval, and we can write

$$H_0 = \beta(T_0 - T) \quad (9)$$

where the temperature coefficient, β , for the present system has been determined to be $\beta = 5 \times 10^6 \text{ K}^{-1} \text{ m}^{-1}$.¹² T_0 is the balanced temperature, where $H_0 = 0$, which for the present system is around 37 °C (corrected for the NaCl effect).¹¹ Approximating that $\langle H \rangle \approx H_0$, gives us a (semi)quantitative relation for the temperature dependence of the Euler characteristic density:

$$\chi_E(T)/A \approx \beta(T_0 - T)/(2\pi l) \quad (10)$$

which implies that χ_E should become increasingly negative with increasing temperature ($T > T_0$), corresponding to an increasing number of passages. This is consistent with the observation that with increasing temperature we are moving further away from the lamellar phase with its planar bilayers. Forming a passage between two bilayer patches involves a bilayer fusion that is often a very slow process on a molecular time scale.^{19,20}

We, therefore, suggest that the second relaxation process of the equilibration after a temperature jump involves the creation of additional passages, changing the topology of the bilayer. We associate a relaxation time τ_t with the topology change, while the collective diffusion process, which relaxes the bilayer concentration, has a relaxation time τ_D . From the data, we conclude that the relaxation time τ_t has a much stronger concentration dependence than τ_D . At low concentrations, $\tau_t \gg \tau_D$, while at high concentrations, we have the opposite situation, $\tau_t \ll \tau_D$. This two-step mechanism involves first a topological change, which then is followed by a collective diffusion process

that redistributes the bilayer material in space. The first, membrane fusion process is a local process, which only changes the bilayer concentrations at short length scales and, therefore, does not directly influence the structure factor for small q and the measured scattering intensity. The change in the structure factor results from the collective diffusion process.

Following the reasoning above, we expect that a T jump, ΔT , should cause a topology change of the order

$$\chi_E(T + \Delta T) - \chi_E(T) \cong -\Delta T \beta A / (2\pi l) \quad (11)$$

As long as the temperature jump involves a perturbation that is small enough, we expect a linear response, and the observed single-exponential relaxation is consistent with this limit. This leads to the linear response equation

$$-\frac{d}{dt}\Delta\chi_E(t) = \frac{1}{\tau_t}\Delta\chi_E(t) \quad (12)$$

for the relaxation of the topology away from the equilibrium value. Using the assumption that the Fourier components, f_q , of the density correlation function relax toward instantaneous values, f_q^0 , determined by the topology χ_E of the bilayer, we have

$$\frac{df_q(t)}{dt} = -\frac{1}{\tau_D(q)}[f_q(t) - f_q^0(\Delta\chi_E)] \quad (13)$$

assuming that τ_D is independent of topology. In a linear expansion

$$f_q^0(\Delta\chi_E) = f_q^0(0) + k\Delta\chi_E \quad (14)$$

with the excess scattered intensity proportional to $f_q(t)$, we find a predicted time dependence of the scattering intensity using the initial condition $f_q^0[\Delta\chi_E(0)] = f_q(0)$ to be

$$I_q(t) = I_q(0) + \Delta I_q \left(1 - \frac{1}{\tau_t - \tau_D(q)} \{ \tau_t \exp(-t/\tau_t) - \tau_D(q) \exp[-t/\tau_D(q)] \} \right) \quad (15)$$

ignoring the term representing the overall cooling of the sample. Equation 15 describes a monotonic relaxation of the signal in the two limits, $\tau_D \gg \tau_t$ and $\tau_t \gg \tau_D$, where a single-exponential relaxation is determined by the slowest relaxation process. In the intermediate regime, $\tau_D \approx \tau_t$, the equation predicts a deviation from the single relaxation behavior. However, for the special case of equal relaxation times, eq 15 implies

$$I(t) = I(0) + \Delta I [1 - \exp(-t/\tau_D) (1 + t/\tau_D)] \quad (16)$$

which is obtained in the limit $\tau_D \rightarrow \tau_t$.

At present, we do not attempt to analyze the crossover region in detail. More systematic experiments are needed to fully describe the complex behavior in this regime. We note, however, that the delicate simultaneous change of the sign of the numerator and denominator as the relaxation times change relative size indicates that small terms, which we have ignored above, might have a qualitative effect in this region of parameter space. In fact, by assuming that the topology relaxation also depends on the density correlation so that eq 12 is generalized to

$$\frac{d}{dt}\Delta\chi_E(t) = -\frac{1}{\tau_t}\Delta\chi_E(t) + \alpha\Delta f_q(t) \quad (17)$$

one can obtain a qualitatively different behavior for $I_q(t)$ around $\tau_t \approx \tau_D$. For $k\alpha < 0$, we find

$$I_q(t) = I(0) + \Delta I_q \left\{ 1 - e^{-\lambda_0 t} \left[\cos(\lambda_1 t) + \frac{\lambda_0}{\lambda_1} \sin(\lambda_1 t) \right] \right\} \quad (18)$$

where

$$\lambda_0 = -\frac{1}{2} \left(\frac{1}{\tau_t} + \frac{1}{\tau_D} \right) \quad (19a)$$

and

$$\lambda_1 = \left[-\frac{k\alpha}{\tau_D} - \left(\frac{1}{\tau_t} - \frac{1}{\tau_D} \right)^2 \right]^{1/2} \quad (19b)$$

when $-k\alpha/\tau_D > (1/\tau_t - 1/\tau_D)^2$. The response in eq 18 is a damped oscillation and results in a nonmonotonic approach to equilibrium. As illustrated in Figure 4, we do observe overshoots for some samples and the existence of a nonmonotonic $I(t)$ clearly depends on the ratio τ_t/τ_D , which varies with q for a given T jump experiment. The coupling term introduced in eq 17 qualitatively accounts for our observations.

Watson and Porte⁹ have also studied the dynamics of a sponge phase using the temperature jump technique. They find a relaxation behavior that is qualitatively different from the one reported in the present work. They studied the system brine–cetyl pyridinium bromide–hexanol, and with an ionic surfactant, the electrical discharge used to generate the T jump can also perturb the bilayers directly. This might be one source of the observed difference in relaxation behavior for the two systems.

A major result of the present experimental study is the observation of an extraordinarily strong concentration dependence of the relaxation time τ_t , which is also coupled with a very strong temperature dependence of the relaxation process. A change in topology of the bilayer implies a fusion/fission process. We have performed independent kinetic experiments on the same system at lower temperatures, at which the equilibration between a droplet of oil in water microemulsion and a two-phase with excess oil is slow. In this case, the monolayers covering the droplets do not fuse on the time scale of minutes and even hours. This is in fact a necessary condition for the use of the surfactant to stabilize emulsions. However, from a model analysis based on calculations of the curvature energy, Kabalnov and Wennerström²¹ concluded that the rate of the monolayer fusion process was strongly dependent on the spontaneous curvature of the surfactant film. Kabalnov and Weers²² further demonstrated experimentally on a $C_{12}E_5$ –oil–water system that the rate of fusion dramatically changes as one tunes the spontaneous curvature close to the balanced point.

In the sponge phase, the topology is much more complex, with a length scale inversely proportional to the volume fraction of the bilayer. At present, we do not have a detailed model for the fusion/fission process of this rather complex structure. We note, however, that Watson and Porte⁹ provide an argument that the topology relaxation time should scale as Φ^{-3} and that Milner et al.²³ estimated the barrier for the fusion to be 5 kT. There is an obvious discrepancy between these estimates and the experimentally observed values.

5. Concluding Remarks

We report the result of an extensive T -jump study focusing on the relaxation behavior of a sponge phase. The temperature

jump results in a single-exponential increase of the light-scattering intensity with time at low (region I, $\Phi_m = 0.22$) and high (region II, $\Phi_m = 0.3$) concentrations. The structural relaxation of the sponge phase following the temperature jump involves (at least) two steps. First, there is a topological change in which patches of membranes fuse to form additional passages with a relaxation time τ_t . Then, the bilayer is rearranged in space by a diffusion process having a relaxation time τ_D . The relaxation times τ_t and τ_D have very different concentration dependences. At lower concentrations, the topology relaxation is the rate-determining step, while at higher concentrations, the rate is limited by the collective diffusion. A major result is the enormous concentration dependence of τ_t , which varies by 3 orders of magnitude when the concentration is changed only by a factor of 2. The reason for this enormous concentration dependence remains to be solved. Work is presently underway to understand better the nonmonotonic light-scattering response in the intermediate concentration range (region III, $0.22 < \Phi_m < 0.30$).

Acknowledgment. We thank Dr. Christian Ikier for help in setting up the T jump and preliminary measurements. This research was supported by the Swedish Natural Science Research Council (NFR).

References and Notes

- (1) Porte, G.; Appell, J.; Bassereau, P.; Marignan, J. *J. Phys. Fr.* **1989**, *50*, 1335–1347.
- (2) Roux, D.; Coulon, C.; Cates, M. E. *J. Phys. Chem.* **1992**, *96*, 4174–4187.
- (3) Strey, R.; Jahn, W.; Porte, G.; Bassereau, P. *Langmuir* **1990**, *6*, 1635–1639.
- (4) Olsson, U.; Wennerström, H. *Adv. Colloid Interface Sci.* **1994**, *49*, 113–146.
- (5) Anderson, D.; Wennerström, H.; Olsson, U. *J. Phys. Chem.* **1989**, *93*, 4243–4253.
- (6) Wennerström, H.; Olsson, U. *Langmuir* **1993**, *9*, 365–368.
- (7) Snabre, P.; Porte, G. *Europhys. Lett.* **1990**, *13*, 641–645.
- (8) Diat, O.; Roux, D. *Langmuir* **1995**, *11*, 1392–1395.
- (9) Waton, G.; Porte, G. *J. Phys. II Fr.* **1993**, *3*, 515–530.
- (10) Schwarz, B.; Mönch, G.; Ilgenfritz, G.; Strey, R. *Langmuir* **2000**, *16*, 8643–8652.
- (11) Le, T. D.; Olsson, U.; Wennerström, H.; Rathke, B.; Uhrmeister, P.; Strey, R. *Phys. Chem. Chem. Phys.* **2001**, *16*, 4346–4354.
- (12) Le, T. D.; Olsson, U.; Wennerström, H.; Schurtenberger, P. *Phys. Rev. E* **1999**, *60*, 4300–4309.
- (13) Olsson, U.; Schurtenberger, P. *Langmuir* **1993**, *9*, 3389–3394.
- (14) Mayer, W.; Woermann, D. *J. Phys. Chem.* **1988**, *92*, 2036–2039.
- (15) Mayer, W.; Woermann, D. *J. Chem. Phys.* **1990**, *93*, 4349–4356.
- (16) Eigen, M.; De Maeyer, L. *Relaxation Methods*. In *Techniques of Organic Chemistry*; Weissberger, A., Ed.; Wiley-Interscience: New York, 1963; Vol. VIII, pp 895–1005.
- (17) Uhrmeister, P. Diplomarbeit, Universität zu Köln, Köln, Germany, 1998.
- (18) Hyde, S.; Andersson, S.; Larsson, K.; Blum, Z.; Landh, T.; Lidin, S.; Ninham, B. W. *The Language of Shape (The Role of Curvature in Condensed Matter: Physics, Chemistry and Biology)*; Elsevier: Amsterdam, 1997.
- (19) Chernomordik, L. V.; Melikyan, G. B.; Chizmadzhev, Y. A. *Biochim. Biophys. Acta* **1987**, *1987*, 309–352.
- (20) Siegel, D. P. *Biophys. J.* **1993**, *65*, 2124–2140.
- (21) Kabalnov, A.; Wennerström, H. *Langmuir* **1996**, *12*, 276–292.
- (22) Kabalnov, A.; Weers, J. *Langmuir* **1996**, *12*, 1931–1935.
- (23) Milner, S. T.; Cates, M. E.; Roux, D. *J. Phys. Fr.* **1990**, *51*, 2629–2639.